Composite Scintillating Nanofibers by Electrospinning for Radiation Detection

Áureo Capuma Ucuanjongo, id11632

April 2025

Indice

1. Introduction

This research work focuses on the development of advanced nanofibers to revolutionize radiation detection and dosimetry. The increasing need for more sophisticated radiation monitoring for medical applications as well as in various contexts demands more precise and adaptable detection solutions. This investigation proposes the creation of hybrid composite nanofibers, combining organic scintillators (such as anthracene, stilbene and others) and inorganic scintillator nanoparticles (such as BaF_2) incorporated into biopolymer matrices. The electrospinning technique will be employed to produce these nanofibers, offering a versatile and low-cost manufacturing approach. The aim is to overcome the limitations of traditional scintillators, which often present disadvantages such as rigidity, toxicity, and sensitivity to environmental factors. The resulting nanofibers will be designed to be flexible, biocompatible, and environmentally friendly, aligning with the principles of the circular economy using recyclable polymers. The intended applications for these nanofibers include large-area radiation detection, non-conventional geometry radiation sensors, and dosimeters. To this end, a systematic investigation of the structural, optical, electrical, and scintillation properties of the nanofibers will be conducted, with the goal of producing a flexible, innovative, and practical fiber mat for radiation detection.

It is expected that this research will contribute to a better understanding of the state of the art in high-energy radiation detection and provide relevant information for the development of new, more efficient materials and detectors for applications in Medical Physics

2. State of the Art

Methods of radiation detection and measurement have been devised that have been successful at providing quantitative data for the purposes of radiation protection of individuals[1]. However, as knowledge of the interaction of radiation with matter (biological matter in particular) has increased, so the need to both understand and measure the deposition of dose in greater detail has increased correspondingly. For example, the medical treatment of patients with more precise radiation probes, the need to detect radiation in non-conventional surfaces such as the human body or in wearable devices and the detection of different varieties of energetic charged particles presents challenges that need to be addressed.

In this respect, the aim of the project is to develop hybrid functionalized radiosensitive nanofibers for radiation detection and dosimetry, based on the combination of organic scintillator compounds and inorganic scintillator nanoparticles with high scintillation responses, embedded inside biopolymers, to form composite high aspect ratio nanofibers, produced by the versatile low-cost electrospinning technique. This is an aspect poorly explored in composite nanofiber systems, and is particularly useful for radiation sensing and dosimetry[1]. Additionally, we intend to harness the organic scintillators response, to obtain flexible, biocompatible, environmentally friendly nanofiber mats, capable to be applied in large area radiation detection, non-conventional geometry radiation sensors and/or wearable electronic personal dosimeters, to be applied in radiotherapy, radiology and nuclear medicine, among others. Envisaged properties involve sensitivities from µGy to tens of Gy, heterogeneities <1%, and independence from energy and dose rate.

Scintillation is the phenomenon of luminescence in solids, fluids or gases, originating at the propagation of the ionizing radiation through them[2]. Currently, most commercial scintillators are inorganic compounds like bismuth germanate ($Bi_4Ge_3O_{12}$-BGO), BaF_2 and Cesium Iodide, activated with Tellurium (CsI:Tl), among other[1][3]. They exhibit excellent scintillation properties, but generally suffer from shortcomings such as harsh fabrication conditions, high costs, toxicity, and sensitivity to humidity and oxygen[4]–[7]. On the other hand, organic scintillators are attracting increasing attention as they have abundant source materials, ease of processing, low cost, and high mechanical flexibility[8]–[10].

Organic scintillators produce light when transversed by a charged particle and they have found use in a wide variety of detectors[1], [9]. The detectors show many desirable qualities as compared to inorganics, particular for human body dosimetry, including water equivalence, energy independence, reproducibility, dose linearity, resistance to radiation damage, and small-volume

high special resolution[7],[11]. They can be broadly categorized into four types: single crystal, liquid, plastic, and glass[12]. The most useful scintillators produce photons with wavelengths between 370-750 nm (blue to red), typically peaking at 425 nm[13] via a series of processes that are initialized when charged particles interact with the material via both excitation and ionization/recombination. Typical photon yields are about 1 photon per 100 eV of energy deposit[14]. Methods to guide the light towards the photon-electron converter, such as diffusive paint, reflectors, photonic crystals, or light guides, may be required to optimize light yield.

The scintillation processes are different for organic and inorganic scintillators. In inorganic scintillators electronic excitation is described as the generation of electron–hole pairs[7]. Their migration and recombination are the key processes in the scintillation.
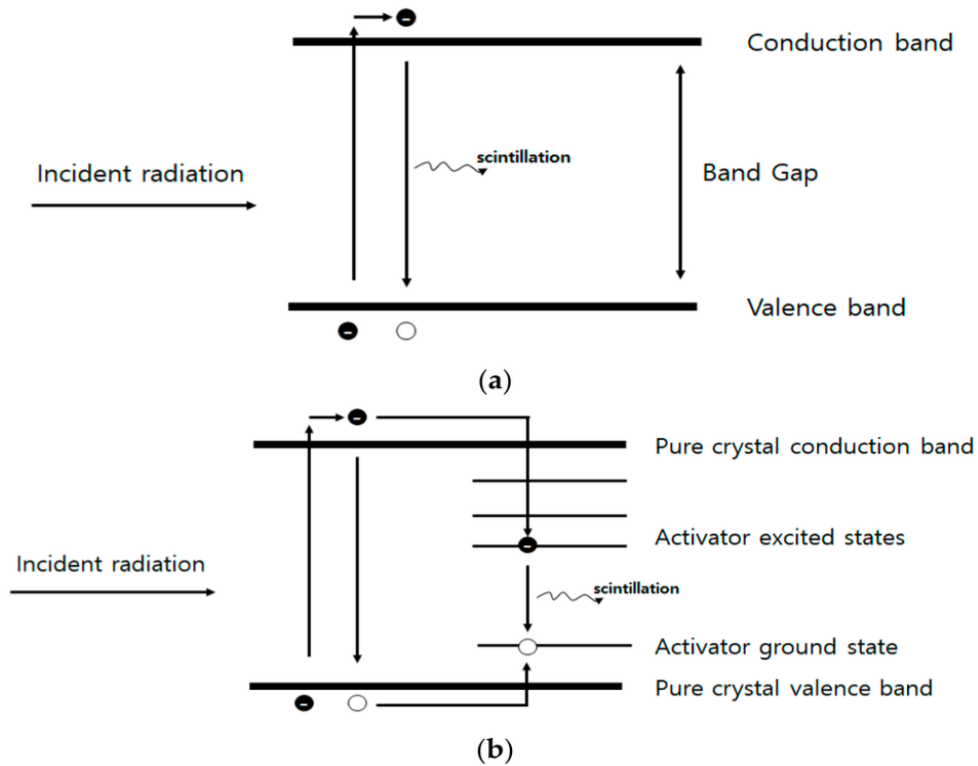

Figure 1- Energy band structure of an inorganic scintillator. (a) Pure crystal (b) Activated crystalline scintillator modified [7]

On the other hand, in organic scintillators the energy of charged particles is absorbed and excites electrons in various molecular states[7]. In particular, both singlet and triplet excited states in organic scintillators play a major role in the dissipation process of the energy deposited by ionizing radiation[10].
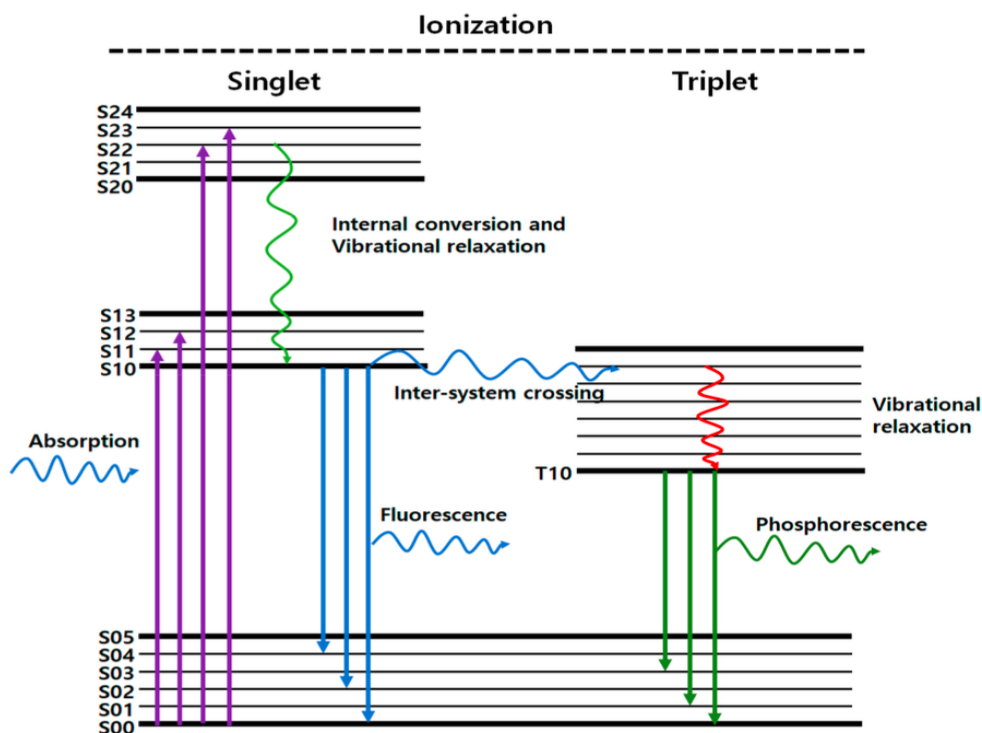
Figure 2- Energy levels of organic molecules modified[7]

Organic scintillators are mainly composed of elements of low atomic numbers, such as H, C, N or O. This is contrary to the cases of inorganic scintillators, which generally contain metal elements of high atomic numbers. Organic scintillators include compounds such as anthracene, stilbene, 1-fenil-3-(2-oxazolil)-benzoxazol (POP) or 1,4-bis[2-(5-phenyl-oxazolyl)]benzene (POPOP)[9]. Anthracene and stilbene crystals have long been used as organic crystalline scintillators. Their light yields have been estimated to be 19 400 and 16 000 photons PER MeV, respectively [15].

Organic scintillators contain H as the main constituent. Hence, using the recoil reaction of protons with fast neutrons, organic scintillators have been used for fast neutron detection[16]. The interaction probability of organic scintillators with high-energy photons such as X-rays and gamma rays is lower than those of inorganic scintillators. On the other hand, their inclusion with BaF_2 and bismuth germanate nanoparticles or metal-free organic X-ray absorbers, such as 4-N-carbazolyl-2,6-dichlorophenyl)bis-(2,4,6-trichlorophenyl)methyl,1,4-bis[2-(5-phenyl-oxazolyl)]benzene, and 2,5-diphenyl-oxazole[17], opens the possibility to develop radiation detectors with larger energy windows. Radiochromic films are a common choice for large-area applications and have been in use for more than 50 years[18]. Currently, Gafchromic (TM) dominates the market, with films for industrial, medical applications and research applications. Their products cover a wide range of

doses from 0.2 Gy to thousands of Gy and can produce measurements with spatial resolutions at the micrometre level. Exposed to radiation the active layer of the films will suffer a visible chromatic alteration proportional to the deposited dose. However, they usually lack the flexibility to conform over large areas and irregular surfaces and are for single use. New flexible detectors need to be developed.

Organic and polymeric scintillators can be easily fabricated in a large-scale, are flexible and can be produced with desired shapes and sizes[19]. The thermoplastic polymers to be used are PET (polyethylene terephthalate), PVC (polyvinyl chloride), PA11 (nylon 1,1), PA66 (nylon 6,6), and PCL (polycaprolactone), each selected for its specific properties and potential applications. PET (polyethylene terephthalate) is widely used in recyclable materials and it has scintillation properties competitive with commercial alternatives [20]. It emits blueish light when exposed to ionizing radiation (PET emission peaks around 370 to 380 nm) [20], [21]. PET has a light yield of 2200 photons/MeV [20] and the decay constant of PET is 7 ns [22]. PVC offers durability and chemical resistance and is commonly used as component material in scintillation detectors [23]. PA11 and PA66 provide high mechanical strength and thermal stability, essential for polymeric matrix applications. PCL is a biodegradable polymer, contributing to environmentally friendly material development. Inorganic nanoparticles and organic scintillators can be embedded inside them for further functionalization. The use of these thermoplastic polymers contributes to resource efficiency and waste reduction, key aspects of a circular economy. This approach not only supports sustainability but also enhances the functionality and applicability of these materials in fields such as dosimetry

Electrospinning is a simple, versatile and cost-effective technique that enables the fabrication of continuous, individual or mat assembled oriented fibers at room temperature, with diameters down to 100 nm or below [24]–[28]. Electrospinning is based on the high voltage jet extraction of a polymer solution or melt through a capillary (needle). By mixing nanoparticles or molecules in the polymeric precursor solutions, long, flexible and continuous fibers with functionalized properties (ferroelectric, magnetic, optical or others) are formed[26]–[28][29], [30]. Using suitable collector electrodes, such as rotating drums, highly aligned flexible polymeric nanofibers with embedded organic molecules are attained, resulting in crystalline assemblies that exhibit significantly improved optical properties. These, in turn, can be harnessed for large area radiation detection, non-conventional geometry radiation sensors and wearable personal dosimeters.
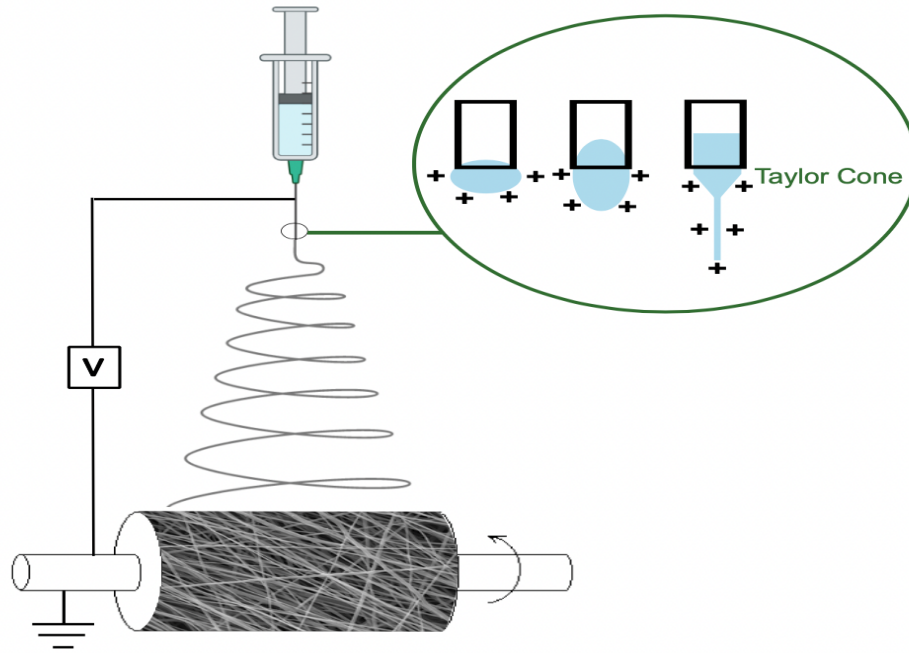
Figura 3- Schematic illustration of the electrospinning setup. Adapted from [31]

In the initial step, the capillary tube is filled with a polymer solution, then a voltage between 1 and 30 kV is applied to the needle to electrify the surface of the polymer solution, which causes polymer droplets to be suspended at the tip of the needle. Once subjected to the electric field, due to the potential difference between the droplet and the collector drum, the droplet is attracted by electrostatic interaction to the collector drum, deforming into a conical geometry known as the Taylor cone [32]–[34]. As the voltage approaches a critical value, the electrostatic forces overcome the surface tension of the droplet, and a charged jet of polymer solution is propelled from the Taylor cone. As the jet travels to the collector, the solvent that makes up the solution evaporates in less than a tenth of a second, and finally, small web-like fibers are collected on the collector [35], [36]. A typical setup for electrospinning is shown in Figure 3.

Once the Taylor cone is formed, there is a possibility that instead of the polymeric jet forming smooth fibers, it will spread into droplets on the collector [37]–[39]. Smooth fibers are created when the Berry number, which is measured by the intrinsic viscosity of the polymer [η] and the concentration c, is greater than a certain critical value c*[η] that is characteristic of the polymer [40]. The specific viscosity of a polymer solution ηsp is calculated by:

$$\eta_{sp} = \frac{\eta_0 - \eta_s}{\eta_s} \tag{1}$$

where η_0 is the viscosity of the solvent and η is the shear viscosity of the polymeric solution at the concentration c.

The properties of the precursor solution and the corresponding processing parameters significantly influence the morphology and characteristics of the electrospun fibers. Key factors include polymer concentration, solvent properties, applied voltage, needle-to-collector distance, flow rate, and environmental conditions.

As polymer concentration or viscosity increases, the average fiber diameter tends to grow. This occurs because the higher viscosity resists elongation, slowing the jet's thinning process. Conversely, low-viscosity solutions often result in thinner fibers or, if the concentration is too low, the formation of droplets instead of continuous fibers (a phenomenon known as electrospraying).
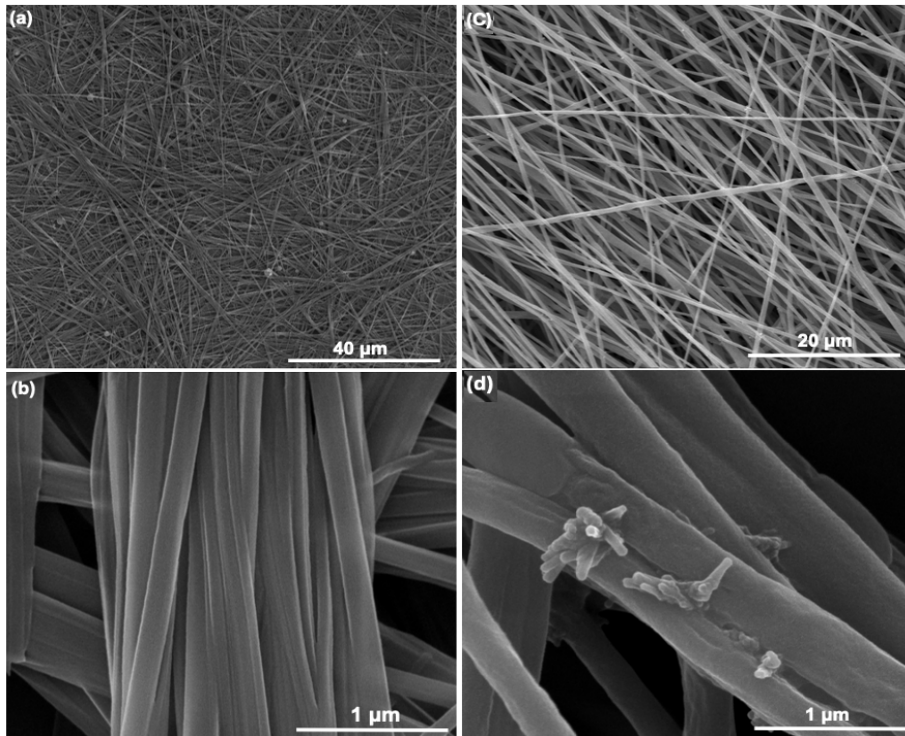

Figure 4 - SEM images of electrospun nanofibers. Adapted from [7]

The critical potential difference V_c required for jet emission, assuming a spherical shape of the droplet at the cone's apex, is given by equation 2 [41]:

$$V_c^2 = 0,36 \left(\frac{D}{L}\right)^2 \left(ln\left(\frac{2L}{R}\right) - \frac{3}{2}\right)(1,3\pi R\gamma) \tag{2}$$

Here, D is the distance over which the high voltage is applied, R is the radius of the syringe needle, L is the length of the fluid column that experiences the accelerating electric field, and γ is the surface tension of the solution. All distances are measured in cm, with the surface tension expressed in dyn/cm, yielding a critical tension, V_C in kV. The applied electric field, determined by the voltage and needle-to-collector distance, must exceed the threshold to initiate jet emission (Equation (1)). For larger electric fields, the fiber diameter tends to increase slightly because more fluid is ejected. However, this effect is less pronounced compared to the influence of solution viscosity.

Solvents with low vapor pressure typically produce thinner fibers. This is because slower solvent evaporation prolongs the jet's elongation and diameter reduction phases before solidification occurs. The choice of solvent also influences the solution's conductivity and surface tension, both of which directly affect fiber formation. Higher solution conductivity increases the electric charge carried by the jet, enhancing the electric elongation force. As a result, the fiber diameter decreases due to increased stretching. Equation (3) illustrates this relationship, where the electric current (I) is proportional to the charge density. In equation 2, the final fiber diameter (d) is determined by the balance between surface tension and the repulsion of surface charges in the stretched jet. At the point where the jet ceases to thin further, the fiber diameter can be expressed as:

$$d_f = \left(\gamma \varepsilon' \left(\frac{Q}{I} \right)^2 \frac{2}{\pi (2 \ln(\chi) - 3)} \right)^{1/3} \qquad (3)$$

where Q is the flow rate of the fluid jet, I is the electric current through the fluid, ε' is the permittivity of the environment (air), γ is the fluid surface tension, and χ is the dimension-less wavelength of the jet's torsional instability (proportional to the curvature radius of the bending perturbation divided by the jet radius).

A shorter needle-to-collector distance reduces the jet's elongation time, resulting in thicker fibers. Conversely, increasing the distance allows more time for jet stretching and solvent evaporation, leading to thinner fibers. On the other hand, excessive distances can weaken the electric field, reducing the stability of fiber formation.

Reducing the needle radius or decreasing the flow rate results in thinner fibers. Smaller needle radii create finer initial jets, while lower flow rates reduce the amount of fluid ejected, enhancing the elongation effect.

In addition to these parameters, the technique is also affected by the environmental conditions, such as the relative humidity and ambient temperature. Higher humidity generally leads to thinner fibers because slower drying allows for extended stretching of the jet. Conversely, excessive humidity can prevent proper drying, causing the jet to break into droplets and inhibiting fiber formation. Similarly, temperature affects solvent evaporation rates, with higher temperatures facilitating faster solidification.

Electrospinning is highly adaptable, enabling the creation of nanofibers with intricate structures by varying needle and collector configurations. In coaxial electrospinning, two needles are concentrically aligned, such that one precursor solution can be delivered through an inner capillary while the other can pass through the outer capillary, creating tubular or core–shell fibers. With side-by-side needles, bi- or three-phase fibers can be obtained [42]. Aligned fibers can be obtained using rotating drums or parallel threads, which is advantageous for applications based on fiber orientation [26], [43], [44]. Using more complex electrodes, such as metallic wires coupled to mobile positioners, liquid collectors, and other assemblies [42], [45], [46], three-dimensional structures can be obtained.

3.Research Proposal

3.1.Objectives

The research aims to develop nanofibers prepared by electrospinning for radiation detectors, focusing on a new generation of composite nanofiber mats embedded with inorganic nanoparticles and organic scintillation materials. The aim is to obtain flexible, biocompatible, environmentally friendly nanofiber mats, capable to be applied in large area radiation detection, non-conventional geometry radiation sensors and/or wearable electronic personal dosimeters. For that, we will use recyclable polymeric and organic compounds as raw material, which will result in environmentally friendly nanofibers framed within the paradigm of a circular economy. The specific objectives are:

1. Synthesis of composite nanofibers embed with organic active compounds such as anthracene, stilbene, fluorescein, 1-fenil-3-(2-oxazolil)-benzoxazol (POP) or 1,4-bis[2-(5-phenyl-oxazolyl)]benzene (POPOP), and X-ray absorbers such as 4-N-carbazolyl-2,6-dichlorophenyl)bis-(2,4,6-trichlorophenyl)methyl and 2,5-diphenyl-oxazole for wide energy radiation detection. Incorporation into the organic polymeric matrix of Polyethylene Terephthalate (PET), polyamide (PA11, PA66), PVC or PCL. Inorganic barium fluoride (BaF_2) or bismuth germanate ($Bi_4Ge_3O_{12}$) nanoparticles will also be used. Systematically characterize the precursor solutions, the synthesis parameters, as well as study and improve the crystallinity in light of their optical and radiation induced responses.

2. Systematic study of the structural, chemical and morphological properties of the composite nanofibers. Of particular relevance is studying and tailoring the inclusions' crystallinity, interfacial structures, and molecular orientation towards improving their optical, nonlinear optical and scintillator responses.

3. Detailed study of the self-assembly properties of the nanoparticles and organic scintillators in electrospun nanofibers, using optical-absorption, dynamic-light-scattering and photoluminescence.

4. Detailed characterization of the static and frequency dependent electric properties and relaxation behavior (electric conductivity, impedance spectroscopy) of the fibers. Determination of the onset of polar order, critical temperatures and activation energies.

5. Systematic study of the optical absorption and photoluminescence of the composite nanofibers. Detailed characterization of their nonlinear optical properties, namely, of their second harmonic generation response.

6. Systematic study of the scintillation response of the individual compounds and composite fibers.

With these studies, the project aims to contribute to the development of innovative scintillating bioorganic active functional materials, towards their application in biocompatible, lightweight, large area or non-conventional geometries precise radiation detectors for flexible, wearable, personal dosimeter systems.

3.2. Work plan

During the candidate Master Thesis, he has already acquired experience, in particular, on the optical characterization of nanostructures, the study of their time-resolved fluorescence and on

fluorescence imaging. Here, the work plan is divided into several complementary tasks, organized by their time evolution:

Task 1: Synthesis radioluminescent electrospun single and composite fibers

The nanofabrication technique that was selected for the production of hybrid polymer and organic/inorganic scintillator composite nanofibers is electrospinning. In this technique, a polymer/radioluminescent precursor solution is extracted under a static electric field ($\sim 10^6$ V/m), applied between a needle metallic tip and a grounded electrode. In-flight, the emitted jet is stretched, the solvent evaporates and the fibers are formed, occurring crystallization of the carrier polymer and of the active molecules/nanoparticles inside it.

The thermoplastic polymers to be used are PET, PVC, PA11, PA66, and PCL, each selected for its specific properties and potential applications as referred in the state of the art. The fabrication of electrospun nanofibers involves the employment of organic scintillators, such as anthracene, stilbene, fluorescein, 1-fenil-3-(2-oxazolil)-benzoxazol (POP) or 1,4-bis[2-(5-phenyl-oxazolyl)]benzene (POPOP), and X-ray absorbers such as 4-N-carbazolyl-2,6-dichlorophenyl)bis-(2,4,6-trichlorophenyl)methyl and 2,5-diphenyl-oxazole for a wide energy window application. These commercially available organic scintillators are economically advantageous and less toxic in comparison to inorganic scintillators. Inorganic scintillators such as BaF_2 and $Bi_4Ge_3O_{12}$ nanoparticles will be also included as they are active in gamma-ray region.

For each scintillator-polymer composite fiber system, detailed optimization and study of the preparation conditions will be performed, namely their precursor solutions, applied electric voltages, solution viscosity, needle feeding rates and collector rotation speeds.

Task 2: Structural, chemical, mechanical and thermal analysis

This part of the work involves a thorough characterization of the prepared fibers. It will provide important feedback information for the electrospinning deposition process. This task is divided into four subtasks:

1) Structural characterization by X-ray diffraction (XRD), using the Brucker D8 diffractometer from CFUM. XRD will allow for the determination of the crystallinity and phases present in the fibers, as well as lattice parameters, strain states and preferential orientations.

2) The detailed morphology and surface characterization of the fibers will be performed by scanning electron microscopy (SEM) and atomic force microscopy (AFM), at CFUM.

Additionally, a deeper study of the local microstructure of initially the scintillator materials and subsequent inclusions in the polymer nanocomposite fibers will be characterized by Cryo-TEM/STEM imaging from an ongoing collaboration with INL in order to obtain information on the morphology and orientation of the radioluminescent inclusions. The suite of scanning/transmission TEM/STEM microscopes coupled with EDX and Electron Energy Loss Spectroscopy (EELS) will enable the identification of oriented growth of the inclusions inside the polymeric fiber matrix and provide both imaging and chemical analysis of the different individual inclusion at the atomic scale, with high spatial resolution.

3) Raman and infrared reflectivity measurements will be performed, at CFUM, to collect complementary information on structural order, stress, and chemical state, before and after the radioluminescent incorporation in the nanofibers.

4) At UMinho, the thermal stability will be evaluated by thermogravimetric analysis (TGA) and differential scanning calorimetry (DSC). The mechanical properties, like Young modulus, will be assessed by dynamic mechanical analysis and uniaxial tensile testing. The hydrophilicity character will be measured by Contact Angle System.

Task 3: Study of the electric properties of the fibers

In this task, dielectric and conductivity measurements will be performed in the composite scintillating nanofibers at CFUM, both in DC and AC. The objective is to access their electrical and dielectric dynamic (AC) response to the applied electric fields, to determine polarization behavior and relaxation phenomena and identify phase transitions (e.g., polymer glass transition, melting) of the fibers. Broadband frequency dependent complex impedance spectroscopy is a powerful technique that distinguishes the intrinsic signal from the extrinsic ones (defects (such as oxygen vacancies), grain boundaries and/or electrode contacts). A detailed quantitative analysis by impedance spectroscopy can separate the leakage, inhomogeneity and parasite capacitance effects, and shed light on the activation energy mechanisms involving organic molecular groups of he samples. As such, these experiments will provide valuable information about the nature of the induced polarization influencing the electrical and optical properties of the system. The work involves the determination of the complex dielectric constant, dielectric modulus and AC conductivity of the nanofibers by impedance spectroscopy, as a function of temperature and frequency. A closed-cycle cryostat and an oven combined with an impedance analyzer will be used for temperature-dependent measurements, covering the range 20-570K. The frequency region is

10Hz-3GHz. DC electrical conductivity and I-V measurements will be performed for different temperatures and applied fields on the same CFUM setups.

Task 4: Optical, luminescent and nonlinear optical properties

The study involves the investigation of the optical properties of the scintillators and electrospun composite fibers, using optical absorption (OA), dynamic light scattering (DLS) and photoluminescence (PL) (fluorescence, phosphorescence) at CFUM. The characterization will extend to the identification of nanocrystalline regions with pronounced luminescence. OA will be carried out using a Shimadzu UV-3600 Plus UV-VIS-NIR spectrophotometer, while PL measurements will be recorded on a Horiba Fluorolog 3 spectrofluorometer.

The non-linear optical second harmonic (SHG) generation performance will be evaluated using a microscope capable of characterizing the polarization dependence of SHG signals generated by individual electrospun composite fibers and matrices, with a spatial resolution of approximately one micrometer. For the second harmonic generation (SHG) measurements, the CFUM mode-locked Ti:sapphire laser, which emits pulses in the near infrared with a duration of 100 fs and a few nano-Joules of energy, will serve as the excitation source. The laser is tunable from 750nm to 950nm. The precision of the sub-micron positioning in the focal plane facilitates the characterization of the non-linear optical response in the transverse direction and along the longitudinal axis of the fiber. This provides valuable information on the spatial distribution and crystal orientations of the fiber and on it non-linear-optical conversion capability.

Task 5: Assessment of the scintillation properties of the nanofibers

Selected groups of samples presenting structural, electrical and optical behavior indicative of the existence of well-organized radioluminescent inclusions inside the polymeric fiber matrix will be measured to determine their scintillating capabilities for radiation sensing. The scintillation nanofiber will be put on the side of a photodiode connected to its controller. The nanofiber-photodiode assembly will be put on a black box to avoid exposure to environmental light. For the excitation, an X-ray source using a Cu cathode, from CFUM, will be used for irradiation of the nanofiber mats. Alternatively, a photomultiplier and associated electronics from CFUM will be used for the scintillation detection. X-ray induced radioluminescence spectra and X-ray photostability will be measure on the fluorescence spectrophotometer with the X-ray source.

We seek to produce a proof-of-concept flexible, wearable and precise radiation detection device for dosimetry, taking advantage of the flexibility and scintillation behavior of the composite nanofiber

mats. Envisaged properties involve sensitivities from μGy to tens of Gy, heterogeneities <1%, and independence from energy and dose rate.

These combined studies will then allow obtaining a deeper knowledge on the role of inorganic nanoparticles and organic scintillator inclusions in improving the radiation induced optical responses of the nanofibers. They will also allow taking advantage of their optical and scintillator behavior to develop new large area radiation detectors, non-conventional geometry radiation sensors and wearable personal dosimeter systems.

3.3. Research proposal timeline

The proposed timeline for this research is presented in Figure 4. As substantiated in the experimental phase of this investigation, it begins with the synthesis of the composition that will be subsequently used in the electrospinning process to produce the nanofibers. Following the fabrication phase, a comprehensive characterization will be performed, including structural, chemical, mechanical, thermal, and electrical analyses, to further examine the resulting materials, as well as the study of second harmonic generation of the nanofibers. Finally, the scintillation properties of the nanofibers will be examined and optimized to obtain flexible fiber mats for ionizing radiation detection.

Task	Task Denomination	Year 1 (1–12)	Year 2 (13–24)	Year 3 (25–36)	Year 4 (37–48)
1	Synthesis radio electrospun single and composite fibers	████████████	████████████	████████████	██████░░
2	Structural, chemical, mechanical and thermal analysis	░███████████	████████████	████████████	████████
3	Study of the electric properties of the fibers	░░██████████	████████████	████████████	██████████
4	Optical, luminescent and nonlinear optical properties	░░░░░░██████	████████████	████████████	██████████░
5	Assessment of the scintillation properties of the nanofibers	░░░░░░░░░░░█	████████████	████████████	████████████

M1 — 1st Progress Report M2 — 2st Progress Report M3 M4 — Thesis

M1	*Electrospinning of Nanofibers*	By the end of the first year several sets of samples with promising electrical and optical results will have been characterized, leading to the beginning of the scintillation measurements.
M2	**Beginning of scintillation measurements**	Control of the best experimental Electrospinning parameters involved in the nanofabrication of aligned scintillation nanofiber arrays.
M3	*Scintillation nanofibers*	Quantitative measurements of the scintillation properties of nanofibers according to their composition will have been attained. From this point on the, the scintillator response of the combinations of polymer+inclusions will be optimized
M4	*Assessment of results*	By the end of the project the PhD thesis will be delivered and a proof-of-concept prototype radiation detector will be delivered.

Figure 4- Research proposal timeline for the project

References

[1]   K. Matuszewski, H. Szweda, P. Cegła, D. Radomiak, and B. Pawałowski, "Program zapewnienia kontroli jakości w medycynie nuklearnej . Testy podstawowe kontroli jakości skanerów PET i PET / CT Quality Assurance in Nuclear Medicine . Routine tests of quality control of PET and PET / CT systems," vol. 8, pp. 459–465, 2019.

[2]   N. Rivera and I. Kaminer, "Light – matter interactions with photonic quasiparticles."

[3]   C. Dujardin *et al.*, "Needs, trends, and advances in inorganic scintillators," *IEEE Trans. Nucl. Sci.*, vol. 65, no. 8, pp. 1977–1997, 2018.

[4]   A. Jana *et al.*, "Perovskite: Scintillators, direct detectors, and X-ray imagers," *Mater. Today*, vol. 55, no. May, pp. 110–136, 2022.

[5]   J. W. Yuan *et al.*, "Highly Efficient Stable Luminescent Radical-Based X-ray Scintillator," *J. Am. Chem. Soc.*, vol. 145, no. 49, pp. 27095–27102, 2023.

[6]   S. Liang *et al.*, "Recent Advances in Synthesis, Properties, and Applications of Metal Halide Perovskite Nanocrystals/Polymer Nanocomposites," *Adv. Mater.*, vol. 33, no. 50, pp. 1–36, 2021.

[7]   S. Min, H. Kang, B. Seo, J. Cheong, C. Roh, and S. Hong, "A review of nanomaterial based scintillators," *Energies*, vol. 14, no. 22, pp. 1–43, 2021.

[8]   M. Chen, C. Wang, and W. Hu, "Organic photoelectric materials for X-ray and gamma ray detection: mechanism, material preparation and application," *J. Mater. Chem. C*, vol. 9, no. 14, pp. 4709–4729, 2021.

[9]   M. Koshimizu, "Recent progress of organic scintillators," *Jpn. J. Appl. Phys.*, vol. 62, no. 1, 2023.

[10]   X. Wang *et al.*, "Organic phosphors with bright triplet excitons for efficient X-ray-excited luminescence," *Nat. Photonics*, vol. 15, no. 3, pp. 187–192, 2021.

[11]   A. S. Beddar, "Plastic scintillation dosimetry and its application to radiotherapy," *Radiat. Meas.*, vol. 41, no. SUPPL. 1, pp. 124–133, 2006.

[12]   J. S. Carlson, P. Marleau, R. A. Zarkesh, and P. L. Feng, "Taking Advantage of Disorder: Small-Molecule Organic Glasses for Radiation Detection and Particle Discrimination," *J. Am.*

Chem. Soc., vol. 139, no. 28, pp. 9621–9626, 2017.

[13]   P. A. Zyla *et al.*, "Review of particle physics," *Prog. Theor. Exp. Phys.*, vol. 2020, no. 8, pp. 1–2093, 2020.

[14]   P. D. Group, *R E V I E W OF PARTICLE P H Y S I C S * Particle Data Group*, vol. 794. 1998.

[15]   T. Yanagida, K. Watanabe, and Y. Fujimoto, "Comparative study of neutron and gamma-ray pulse shape discrimination of anthracene, stilbene, and p-terphenyl," *Nucl. Instruments Methods Phys. Res. Sect. A Accel. Spectrometers, Detect. Assoc. Equip.*, vol. 784, pp. 111–114, 2015.

[16]   F. B. Darby *et al.*, "Neutron-Gamma Noise Measurements in a Zero-Power Reactor Using Organic Scintillators," *IEEE Trans. Nucl. Sci.*, vol. 71, no. 5, pp. 1033–1040, 2024.

[17]   A. Luo *et al.*, "Efficient metal free organic radical scintillators," *Nat. Commun.* , vol. 15, no. 1, pp. 1–8, 2024.

[18]   M. J. Butson, P. K. N. Yu, T. Cheung, and P. Metcalfe, "Radiochromic film for medical radiation dosimetry," *Mater. Sci. Eng. R Reports*, vol. 41, no. 3–5, pp. 61–120, 2003.

[19]   Y. N. Kharzheev, "Scintillation counters in modern high-energy physics experiments," *Phys. Part. Nucl.*, vol. 46, no. 4, pp. 678–728, 2015.

[20]   H. Nakamura, Y. Shirakawa, S. Takahashi, and H. Shimizu, "Evidence of deep-blue photon emission at high efficiency by common plastic," *Epl*, vol. 95, no. 2, pp. 0–3, 2011.

[21]   H. Nakamura *et al.*, "Blended polyethylene terephthalate and polyethylene naphthalate polymers for scintillation base substrates," *Radiat. Meas.*, vol. 59, pp. 172–175, 2013.

[22]   J. W. Wetzel, E. Tiras, B. Bilki, O. Koseyan, N. Bostan, and Y. Onel, "Measuring the Scintillation Decay Constant of Pen and PET with 120 GeV Proton Beam Excitation," *2020 IEEE Nucl. Sci. Symp. Med. Imaging Conf. NSS/MIC 2020*, pp. 1–2, 2020.

[23]   D. Mulmule *et al.*, "A plastic scintillator array for reactor based anti-neutrino studies," *Nucl. Instruments Methods Phys. Res. Sect. A Accel. Spectrometers, Detect. Assoc. Equip.*, vol. 911, no. September, pp. 104–114, 2018.

[24]   M. Ahmadi Bonakdar and D. Rodrigue, "Electrospinning: Processes, Structures, and Materials," *Macromol*, vol. 4, no. 1, pp. 58–103, 2024.

[25]   J. Xue, T. Wu, Y. Dai, and Y. Xia, "Electrospinning and electrospun nanofibers: Methods,

materials, and applications," *Chem. Rev.*, vol. 119, no. 8, pp. 5298–5415, 2019.

[26]   M.–nitroaniline Electrospun *et al.*, "Oriented Single-Crystal-like Molecular," vol. 5, no. 1, pp. 73–78, 2011.

[27]   P. Sá *et al.*, "Ferroelectric characterization of aligned barium titanate nanofibres," *J. Phys. D. Appl. Phys.*, vol. 46, no. 10, 2013.

[28]   R. M. F. Baptista *et al.*, "Self-assembly of dipeptide Boc-diphenylalanine nanotubes inside electrospun polymeric fibers with strong piezoelectric response," *Nanoscale Adv.*, vol. 1, no. 11, pp. 4339–4346, 2019.

[29]   V. Bayzi Isfahani *et al.*, "Flexible Magnetocaloric Fiber Mats for Room-Temperature Energy Applications," *ACS Appl. Mater. Interfaces*, vol. 16, no. 7, pp. 8655–8667, 2024.

[30]   D. Santos *et al.*, "Bioinspired Cyclic Dipeptide Functionalized Nanofibers for Thermal Sensing and Energy Harvesting," *Materials (Basel).*, vol. 16, no. 6, 2023.

[31]   D. Santos *et al.*, "Nanostructured Electrospun Fibers with Self-Assembled," 2023.

[32]   A. Vaseashta, "Controlled formation of multiple Taylor cones in electrospinning process," *Appl. Phys. Lett.*, vol. 90, no. 9, 2007.

[33]   X. Zhang, L. Xie, X. Wang, Z. Shao, and B. Kong, "Electrospinning super-assembly of ultrathin fibers from single- to multi-Taylor cone sites," *Appl. Mater. Today*, vol. 26, p. 101272, 2022.

[34]   A. L. Yarin, S. Koombhongse, and D. H. Reneker, "Taylor cone and jetting from liquid droplets in electrospinning of nanofibers," *J. Appl. Phys.*, vol. 90, no. 9, pp. 4836–4846, 2001.

[35]   X. Hu, S. Liu, G. Zhou, Y. Huang, Z. Xie, and X. Jing, "Electrospinning of polymeric nanofibers for drug delivery applications," *J. Control. Release*, vol. 185, no. 1, pp. 12–21, 2014.

[36]   N. Bhardwaj and S. C. Kundu, "Electrospinning: A fascinating fiber fabrication technique," *Biotechnol. Adv.*, vol. 28, no. 3, pp. 325–347, 2010.

[37]   A. Kaltbeitzel *et al.*, "STED Analysis of Droplet Deformation during Emulsion Electrospinning," *Macromol. Chem. Phys.*, vol. 218, no. 9, pp. 1–13, 2017.

[38]   H. Xu, L. Wang, and X. Qin, "A study on the droplet-jet electrospinning modes: Dynamic

behavior and control theory," *Phys. Fluids*, vol. 37, no. 1, 2025.

[39]   J. Vonch, A. Yarin, and C. M. Megaridis, "Electrospinning: A study in the formation of nanofibers," *J. Undergrad. Res. Univ. Illinois Chicago*, vol. 1, no. 1, 2007.

[40]   Y. Dzenis, "Spinning continuous fibers for nanotechnology," *Science (80-.).*, vol. 304, no. 5679, pp. 1917–1919, 2004.

[41]   B. Sun *et al.*, "Advances in three-dimensional nanofibrous macrostructures via electrospinning," *Prog. Polym. Sci.*, vol. 39, no. 5, pp. 862–890, 2014.

[42]   J. D. Starr and J. S. Andrew, "Janus-type bi-phasic functional nanofibers," *Chem. Commun.*, vol. 49, no. 39, pp. 4151–4153, 2013.

[43]   Y. Jiang, M. Zhou, Z. Shen, X. Zhang, H. Pan, and Y. H. Lin, "Ferroelectric polymers and their nanocomposites for dielectric energy storage applications," *APL Mater.*, vol. 9, no. 2, 2021.

[44]   A. Koka and H. A. Sodano, "High-sensitivity accelerometer composed of ultra-long vertically aligned barium titanate nanowire arrays," *Nat. Commun.*, vol. 4, 2013.

[45]   G. Luo, K. S. Teh, Y. Liu, X. Zang, Z. Wen, and L. Lin, "Direct-Write, Self-Aligned Electrospinning on Paper for Controllable Fabrication of Three-Dimensional Structures," *ACS Appl. Mater. Interfaces*, vol. 7, no. 50, pp. 27765–27770, 2015.

[46]   H. Y. Kim, M. Lee, K. J. Park, S. Kim, and L. Mahadevan, "Nanopottery: Coiling of electrospun polymer nanofibers," *Nano Lett.*, vol. 10, no. 6, pp. 2138–2140, 2010.